Development 140, 423-432 (2013) doi:10.1242/dev.081927

Roles of Bmp4 during tooth morphogenesis and sequential tooth formation

Shihai Jia[1,3,*], Jing Zhou[1,3,*], Yang Gao[3], Jin-A Baek[3,‡], James F. Martin[4], Yu Lan[1,2,3] and Rulang Jiang[1,2,3,§]

SUMMARY

Previous studies have suggested that Bmp4 is a key Msx1-dependent mesenchymal odontogenic signal for driving tooth morphogenesis through the bud-to-cap transition. Whereas all tooth germs were arrested at the bud stage in *Msx1*$^{-/-}$ mice, we show that depleting functional *Bmp4* mRNAs in the tooth mesenchyme, through neural crest-specific gene inactivation in *Bmp4*$^{f/f}$*;Wnt1Cre* mice, caused mandibular molar developmental arrest at the bud stage but allowed maxillary molars and incisors to develop to mineralized teeth. We found that expression of *Osr2*, which encodes a zinc finger protein that antagonizes Msx1-mediated activation of odontogenic mesenchyme, was significantly upregulated in the molar tooth mesenchyme in *Bmp4*$^{f/f}$*;Wnt1Cre* embryos. *Msx1* heterozygosity enhanced maxillary molar developmental defects whereas *Osr2* heterozygosity partially rescued mandibular first molar morphogenesis in *Bmp4*$^{f/f}$*;Wnt1Cre* mice. Moreover, in contrast to complete lack of supernumerary tooth initiation in *Msx1*$^{-/-}$*Osr2*$^{-/-}$ mice, *Osr2*$^{-/-}$*Bmp4*$^{f/f}$*;Wnt1Cre* compound mutant mice exhibited formation and subsequent arrest of supernumerary tooth germs that correlated with downregulation of *Msx1* expression in the tooth mesenchyme. In addition, we found that the Wnt inhibitors Dkk2 and Wif1 were much more abundantly expressed in the mandibular than maxillary molar mesenchyme in wild-type embryos and that *Dkk2* expression was significantly upregulated in the molar mesenchyme in *Bmp4*$^{f/f}$*;Wnt1Cre* embryos, which correlated with the dramatic differences in maxillary and mandibular molar phenotypes in *Bmp4*$^{f/f}$*;Wnt1Cre* mice. Together, these data indicate that Bmp4 signaling suppresses tooth developmental inhibitors in the tooth mesenchyme, including Dkk2 and Osr2, and synergizes with Msx1 to activate mesenchymal odontogenic potential for tooth morphogenesis and sequential tooth formation.

KEY WORDS: Bmp4, Dkk2, Msx1, Osr2, Wnt, Tooth development, Sequential tooth initiation, Mouse

INTRODUCTION

Mammalian tooth development involves highly regulated reciprocal signaling interactions between the epithelium and mesenchyme. Classic tissue recombination experiments demonstrated that, although tooth inductive signals arise initially in the embryonic oral ectoderm, tooth inductive potential shifts from ectoderm to mesenchyme at the early tooth bud stage, with the developing tooth mesenchyme acquiring capability of inducing tooth organogenesis even when combined with non-dental epithelium (Kollar and Baird, 1970; Kollar and Fisher, 1980; Lumsden, 1988; Mina and Kollar, 1987; Ruch et al., 1973). As development proceeds, mesenchymal signals induce formation of an epithelial signaling center, termed the primary enamel knot (PEK), in the distal region of the tooth bud, which in turn drives tooth morphogenesis through the 'cap' and 'bell' stages by signaling into both the dental epithelium and mesenchyme. Many signaling molecules, including members of the Bmp, Fgf and Wnt families and Shh, are expressed during early tooth development (reviewed by Jernvall and Thesleff, 2000; Tucker and Sharpe, 2004; Zhang et al., 2005). Among these, Bmp4 exhibits an expression pattern coinciding with the shift of odontogenic potential from epithelium to mesenchyme during tooth bud formation (Vainio et al., 1993). Bmp signaling is required for activation of expression of the Msx1 transcription factor in the developing tooth mesenchyme (Tucker et al., 1998). In mice lacking *Msx1* gene function, *Bmp4* mRNA expression was downregulated in the tooth mesenchyme and tooth development arrested at the bud stage (Chen et al., 1996; Satokata and Maas, 1994). Addition of recombinant Bmp4 protein rescued *Msx1*$^{-/-}$ mutant mandibular first molar tooth germs to late bell stage in explant cultures (Bei et al., 2000; Chen et al., 1996). Bmp4-releasing beads placed in contact with isolated dental epithelium induced localized expression of a PEK marker p21 (Cdkn1a) (Jernvall et al., 1998). Transgenic *Bmp4* expression driven by an *Msx1* gene promoter also partially rescued *Msx1*$^{-/-}$ mutant first molar tooth germs to the cap stage with formation of a PEK (Zhao et al., 2000). In addition, mice homozygous for *Pax9* null mutations exhibit tooth developmental arrest at the early bud stage accompanied by loss of *Bmp4* and *Msx1* expression in developing tooth mesenchyme (Peters et al., 1998; Zhou et al., 2011). *In vitro* biochemical assays showed that Msx1 and Pax9 act synergistically to activate the *Bmp4* gene promoter (Ogawa et al., 2006). Moreover, tissue-specific inactivation of *Bmpr1a* in epithelial tissues resulted in tooth developmental arrest at the bud stage (Andl et al., 2004; Liu et al., 2005). These data led to the conclusion that Bmp4 is a key Msx1-dependent signal for induction of PEK formation to drive tooth morphogenesis beyond the bud stage (Bei et al., 2000; Miletich et al., 2011; O'Connell et al., 2012; Zhao et al., 2000). However, direct genetic analysis of the requirement for Bmp4 in early tooth morphogenesis has not been documented.

Teeth are iterative structures that form sequentially in an anterior-to-posterior direction but little is known about the molecular mechanisms regulating sequential tooth formation. In

[1]Division of Developmental Biology, Cincinnati Children's Hospital Medical Center, Cincinnati, OH 45229, USA. [2]Division of Plastic Surgery, Cincinnati Children's Hospital Medical Center, Cincinnati, OH 45229, USA. [3]Center for Oral Biology and Department of Biomedical Genetics, University of Rochester School of Medicine and Dentistry, Rochester, NY 14642, USA. [4]Department of Molecular Physiology and Biophysics, Baylor College of Medicine, One Baylor Plaza, Houston, TX 77030, USA.

*These authors contributed equally to this work
‡Present address: Institute of Oral Biosciences and BK21 Program, Chonbuk National University School of Dentistry, Jeonju 561-756, Republic of Korea
§Author for correspondence (rulang.jiang@cchmc.org)

Accepted 5 November 2012

humans, heterozygous loss-of-function mutations in either *MSX1* or *PAX9* cause selective tooth agenesis, which often preferentially affects the posterior molars and second premolars (Stockton et al., 2000; Vastardis et al., 1996; Mostowska et al., 2012). Although mice heterozygous for either *Msx1* or *Pax9* do not exhibit tooth defects, many $Msx1^{+/-}Pax9^{+/-}$ compound heterozygous mice lack third molars (Nakatomi et al., 2010). Interestingly, transgenic *Bmp4* expression driven by the mouse *Msx1* gene promoter rescued the tooth defects in $Msx1^{+/-}Pax9^{+/-}$ compound heterozygous mice (Nakatomi et al., 2010). Moreover, whereas mice lacking the Osr2 transcription factor develop uniquely supernumerary teeth lingual to their molar teeth, supernumerary tooth formation in the $Osr2^{-/-}$ mice is accompanied by lingual expansion of the domain of *Bmp4* mRNA expression in the tooth mesenchyme (Zhang et al., 2009). Remarkably, in contrast to early tooth developmental arrest in $Msx1^{-/-}$ mutant mice, mice lacking both Msx1 and Osr2 showed continued first molar morphogenesis to the late bell stage, accompanied by partially restored mesenchymal *Bmp4* expression. However, the $Msx1^{-/-}Osr2^{-/-}$ double mutant mice did not develop supernumerary or mandibular second molar teeth (Zhang et al., 2009). To directly investigate the roles of Bmp4 in tooth development and sequential tooth formation, we generated and analyzed tooth development in $Bmp4^{f/f}$*;Wnt1Cre* mice in which the *Bmp4* gene is inactivated in neural crest-derived craniofacial mesenchyme, including the tooth mesenchyme. Although mandibular first molar development was arrested at the bud stage, the maxillary first and second molars as well as both upper and lower incisors developed to mineralized teeth in $Bmp4^{f/f}$*;Wnt1Cre* mutant mice. Further generation and analyses of compound mutant mice deficient in either *Msx1* or *Osr2* in the $Bmp4^{f/f}$*;Wnt1Cre* mutant background indicate that Bmp4 signaling suppresses *Osr2* expression and synergizes with Msx1 to drive propagation of mesenchymal odontogenic activity during tooth morphogenesis and sequential tooth formation.

MATERIALS AND METHODS

Mouse strains

The $Bmp4^{f/f}$, $Bmp4^{+/-}$, $Msx1^{+/-}$, $Osr2^{+/-}$ and *Wnt1Cre* transgenic mice have been described previously (Danielian et al., 1998; Lan et al., 2004; Liu et al., 2005; Winnier et al., 1995). The $Bmp4^{+/-}$, $Msx1^{+/-}$ and $Osr2^{+/-}$ mice were maintained in the C57BL/6 background, *Wnt1Cre* mice were maintained in the CD1 background, and the $Bmp4^{f/f}$ mice maintained by sibling intercrosses. The tooth phenotypes were indistinguishable between $Bmp4^{f/f}$*;Wnt1Cre* and $Bmp4^{f/-}$*;Wnt1Cre* mutant mice at various prenatal and postnatal stages examined, hence data were combined.

Histology and skeletal analysis

For histological analysis, embryos were collected from timed pregnant females, fixed in Bouin's fixative or 4% paraformaldehyde (PFA), dehydrated through graded ethanol series, embedded in paraffin, and sectioned at 7 μm thickness. Sections were stained with Hematoxylin and Eosin, or using trichrome staining as described previously (Chen et al., 2009). Skeletons were prepared by using Dermestid beetles as described previously (Hefti et al., 1980).

Immunofluorescence staining and *in situ* hybridization

For immunofluorescence staining and *in situ* hybridization, embryos were fixed in 4% PFA overnight at 4°C and processed for paraffin sections as described above. Indirect immunofluorescence staining was performed as described (Zhou et al., 2011). Anti-phospho-Smad1/5 antibody was purchased from Cell Signaling Technology. *In situ* hybridization of sections was performed as described previously (Zhang et al., 1999). The cRNA probe for *Bmp4* was specific for the exon 4, which was flanked by loxP sites in the $Bmp4^{f}$ allele.

Laser capture microdissection (LCM) and RNAseq

Embryos were dissected on ice, and the heads were frozen immediately in Tissue-Tek OCT compound by immersion in liquid nitrogen. Fresh-frozen tissue was cryosectioned and collected on Arcturus PEN membrane glass slides (Applied Biosystems). The slides were immediately refrozen and stored at −80°C. The tooth mesenchyme tissues were isolated by laser capture microdissection (LCM) using Veritas Laser Microdissection instrument model 704. Maxillary and mandibular molar mesenchyme tissues were each pooled from three embryos of the same genotype and total RNAs extracted by using the RNeasy Micro Kit (Qiagen). cDNA templates were generated by using the NuGEN Ovation RNA-Seq v2 system. Sequencing libraries were generated by using Illumina Nextera DNA Sample Prep Kit and sequenced using Illumina Hiseq 2000. Sequenced reads were mapped to the reference mouse genome (mm9) using Bowtie version 0.12.7. Single-end reads were aligned using Tophat version 1.4.1 for Illumina (Brunskill and Potter, 2012).

RNAseq data analysis

The RNAseq raw data have been deposited into NCBI Gene Expression Omnibus database (http://www.ncbi.nlm.nih.gov/geo) (accession number GSE39918). RNAseq data were analyzed using AvadisNGS software, with the reads per kilobase exon per million mapped sequences (RPKM) value calculated for each RefSeq gene for relative gene expression. For analyses of differential expression, the fold change cut-off was set at 1.5-fold or higher and *P*-values <0.01 from the Audic Claverie test were considered to be statistically significant, with Benjamini Hochberg FDR multiple testing correction (Brunskill and Potter, 2012).

Quantitative real-time RT-PCR

Quantitative PCR amplifications were performed using the C1000 Touch Thermal Cycler (Bio-Rad) and the SsoAdvanced SYBR Green Supermix (Bio-Rad). PCR reaction was run in a program of 95°C for 30 seconds, followed by 40 cycles of 95°C for 5 seconds and 60°C for 30 seconds, with a melt curve generation cycle at the end. PCR reactions were carried out in duplicate and relative levels of mRNAs were normalized to *Hprt* using the standard curve method. Student's *t*-test was used to analyze pair-wise differential expression and a *P*-value <0.05 was considered to be statistically significant.

RESULTS

Tooth developmental defects in $Bmp4^{f/f}$*;Wnt1Cre* mutant mice

Because *Bmp4*-null mouse embryos die prior to embryonic day (E) 9.5 (Winnier et al., 1995), before tooth morphogenesis occurs, we investigated the roles of Bmp4 in tooth development using Cre/loxP-mediated conditional gene inactivation of the $Bmp4^{f}$ allele containing loxP sites flanking exon-4 (Liu et al., 2005). The *Wnt1Cre* transgenic mice express Cre recombinase transiently in premigratory neural crest cells and have been shown to efficiently delete loxP-flanked DNA sequences from neural crest-derived craniofacial mesenchyme, including the developing tooth mesenchyme (Chai et al., 2000; Danielian et al., 1998; Han et al., 2003). Indeed, in contrast to strong *Bmp4* mRNA expression in the developing tooth mesenchyme at E13.5 in control embryos (Fig. 1A), *Bmp4* mRNA was undetectable in the $Bmp4^{f/f}$*;Wnt1Cre* mutant tooth mesenchyme by *in situ* hybridization analyses using cRNA probes specific for the exon-4 sequences (Fig. 1B). To quantify the efficiency of inactivation of the *Bmp4* gene in the tooth mesenchyme, we isolated maxillary and mandibular molar tooth mesenchyme from E13.5 wild-type and $Bmp4^{f/f}$*;Wnt1Cre* mutant littermates using LCM (supplementary material Fig. S1) and compared the levels of exon-4-containing *Bmp4* mRNAs by real-time RT-PCR. The $Bmp4^{f/f}$*;Wnt1Cre* mutant maxillary and mandibular molar tooth mesenchyme each contained <1% of the amount of exon-4-

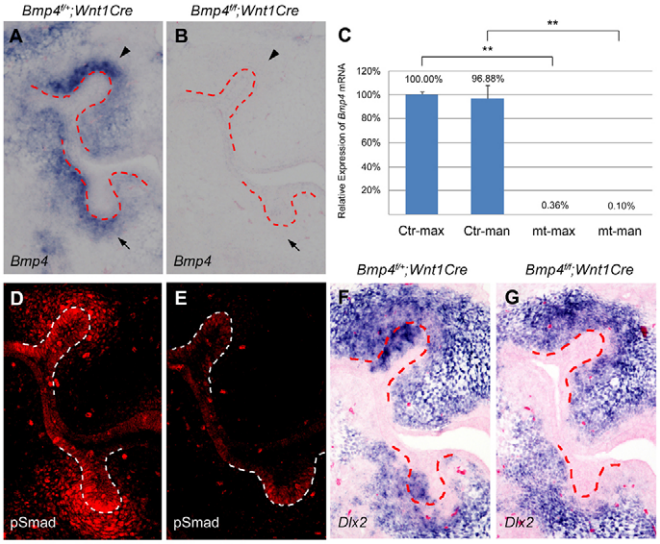

Fig. 1. Loss of *Bmp4* gene activity in the developing tooth mesenchyme in *Bmp4$^{f/f}$;Wnt1Cre* mutant embryos. (**A**,**B**) *Bmp4* mRNA expression in the tooth mesenchyme in E13.5 control (A) and *Bmp4$^{f/f}$;Wnt1Cre* mutant (B) mouse embryos detected using cRNA probes specific for exon-4 sequences. Signal is shown in blue. Dashed line marks the boundary between the dental epithelium and mesenchyme. (**C**) Relative amounts of exon-4-containing *Bmp4* mRNAs in the E13.5 maxillary and mandibular molar mesenchyme in control and *Bmp4$^{f/f}$;Wnt1Cre* mutant embryos. Ctr-max, control maxillary; Ctr-Man, control mandibular; mt-max, mutant maxillary; mt-man, mutant mandibular. The double asterisks indicate significant difference for the pair-wise comparison (P<0.01). Error bars represent s.e.m. (**D**,**E**) Immunofluorescence detection of phospho-Smad1/5 (shown in red) in the first molar tooth germs in E13.5 control (D) and *Bmp4$^{f/f}$;Wnt1Cre* mutant (E) embryos. (**F**,**G**) Comparison of *Dlx2* expression in the first molar tooth germs of E13.5 control (F) and *Bmp4$^{f/f}$;Wnt1Cre* mutant (G) embryos.

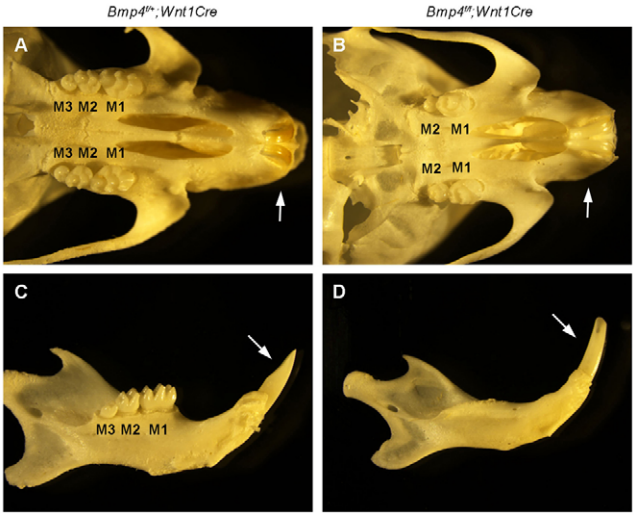

Fig. 2. Tooth phenotype in *Bmp4$^{f/f}$;Wnt1Cre* mutant mice. (**A**,**B**) Skeletal preparations of P21 control (A) and *Bmp4$^{f/f}$;Wnt1Cre* (B) upper jaws. (**C**,**D**) Skeletal preparations of P21 control (C) and *Bmp4$^{f/f}$;Wnt1Cre* (D) lower jaws. M1, M2 and M3 mark the first, second and third molars, respectively. Arrows point to the incisor region.

containing *Bmp4* mRNAs present in the wild-type counterparts (Fig. 1C). Consistent with loss of Bmp4 function in the tooth mesenchyme, little phosphorylated Smad1/5 (pSmad1/5) was detected in the developing tooth mesenchyme in the mutant embryos whereas high levels of pSmad1/5 were present in both the dental epithelium and mesenchyme in the control littermates at E13.5 (Fig. 1D,E). Furthermore, in contrast to strong expression of *Dlx2* mRNA in the buccal side of the developing tooth epithelium in both the maxillary and mandibular molar tooth germs in E13.5 control mouse embryos (Fig. 1F), *Dlx2* mRNA expression was undetectable in the developing upper and lower molar tooth epithelium in the *Bmp4$^{f/f}$;Wnt1Cre* mutant littermates (Fig. 1G). These data indicate that Bmp4 function was effectively inactivated in the neural crest-derived tooth mesenchyme in the *Bmp4$^{f/f}$;Wnt1Cre* mutant mice.

We examined newborn *Bmp4$^{f/f}$;Wnt1Cre* mutant mice for tooth developmental defects by histological analysis. Whereas both maxillary and mandibular first molar tooth germs progressed to the cytodifferentiation stage in the *Bmp4$^{f/+}$;Wnt1Cre* control littermates (supplementary material Fig. S2A,C), *Bmp4$^{f/f}$;Wnt1Cre* mutants showed retarded maxillary first molar tooth germs at the late bell stage and absence of the mandibular first molar tooth germ (supplementary material Fig. S2B,D). We also detected substantially smaller maxillary second molar tooth germs and absence of mandibular second molar tooth germs in the *Bmp4$^{f/f}$;Wnt1Cre* mutants in comparison with the well-developed late-bell stage second molar tooth germs in the control littermates (supplementary material Fig. S2E-H). Although previous studies suggested that Bmp4 is an essential signal downstream of Msx1 in the developing secondary palate (Zhang et al., 2002), we found that only ~16% of the *Bmp4$^{f/f}$;Wnt1Cre* mutant mice examined at late gestation or postnatal day (P) 0 exhibited cleft palate. Indeed, most *Bmp4$^{f/f}$;Wnt1Cre* mutant mice survived postnatally but exhibited postnatal growth retardation by three weeks of age. Skeletal preparations showed that, whereas the control littermates had three well-mineralized molars and one incisor in each quadrant (Fig. 2A,C), the *Bmp4$^{f/f}$;Wnt1Cre* mice had mineralized upper and lower incisors as well as maxillary first and second molars, but completely lacked mandibular molars (Fig. 2B,D). The mutant maxillary molars were smaller with shallower cusps than their counterparts in the control mice. In addition, the mutant mandibular incisors exhibited a round shape, in contrast to the sharp mandibular incisors of the control littermates (Fig. 2C,D). Histological analyses of P5 mouse incisor tooth germs indicate that both the odontoblast and ameloblast layers of the lower incisor tooth germs were malformed, resulting in significantly reduced enamel deposition on the labile surface of the lower incisors in the mutant mice (supplementary material Fig. S3).

We analyzed embryos from E12.5 to E16.5 and found that mandibular first molar development was arrested at the bud stage in the *Bmp4$^{f/f}$;Wnt1Cre* mutant embryos (Fig. 3A-F). By contrast, the maxillary first molar tooth germs in *Bmp4$^{f/f}$;Wnt1Cre* mutant embryos progressed to the cap stage by E14.5, similar to the control littermates (Fig. 3G,H). By E15.5, the mutant maxillary first molar tooth germs were obviously smaller than those in the control littermates (Fig. 3I,J). At E16.5, the maxillary first molar tooth germs continued to expand in size in both control and mutant embryos, but the size and morphology of the mutant maxillary first molar tooth germs appeared similar to the E15.5 control maxillary first molar tooth germs (Fig. 3I-L).

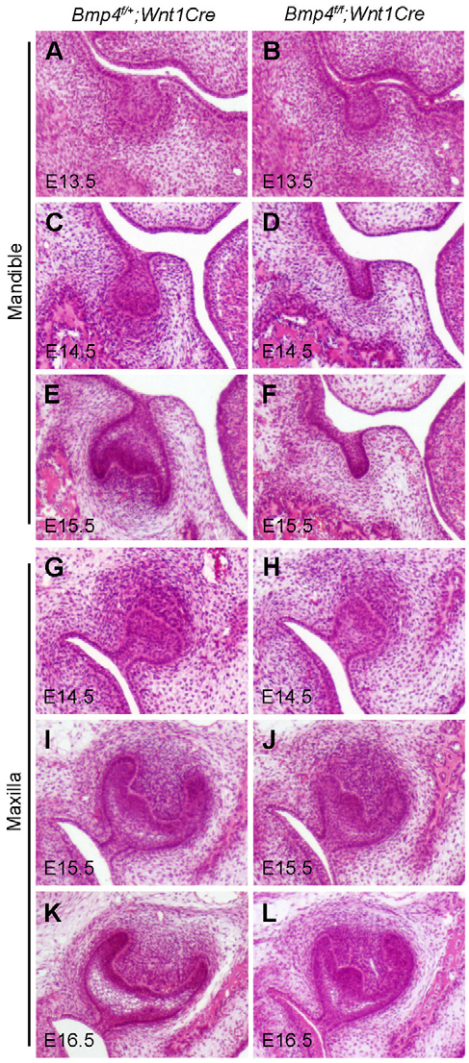

Fig. 3. Molar developmental defects in the *Bmp4$^{f/f}$;Wnt1Cre* embryos. (**A-L**) Hematoxylin and Eosin-stained frontal sections through the developing first molar tooth germs of *Bmp4$^{f/+}$;Wnt1Cre* control (A,C,E,G,I,K) and *Bmp4$^{f/f}$;Wnt1Cre* mutant (B,D,F,H,J,L) mouse embryos from E13.5 to E16.5 are shown.

Tooth developmental arrest in *Msx1*$^{-/-}$ mutant mice could not be fully accounted for by loss of Msx1-dependent *Bmp4* expression in the tooth mesenchyme

Although previous reports have shown significant loss of *Bmp4* mRNA expression in the molar tooth mesenchyme by E13.5 in *Msx1*$^{-/-}$ mutant embryos as detected by *in situ* hybridization (Chen et al., 1996; Zhang et al., 2009), a recent microarray-based gene expression profiling study of LCM-isolated tooth tissues from wild-type and *Msx1*$^{-/-}$ mutant embryos revealed that the levels of *Bmp4* mRNA in the E13.5 *Msx1*$^{-/-}$ mutant mandibular molar tooth mesenchyme was reduced by only ~26% in comparison with the control littermates (O'Connell et al., 2012) (see also ToothCODE database http://compbio.med.harvard.edu/ToothCODE). To directly compare the amount of loss of *Bmp4* mRNA in the *Msx1*$^{-/-}$ versus *Bmp4$^{f/f}$;Wnt1Cre* mutant tooth mesenchyme, we isolated the maxillary and mandibular molar tooth mesenchyme from E13.5 and E14.0 *Msx1*$^{-/-}$ mutant and *Msx1*$^{+/-}$ control littermates using LCM and carried out quantitative real-time RT-PCR analyses of exon-4-containing *Bmp4* mRNAs. We found that the E13.5 *Msx1*$^{-/-}$ mutant maxillary and mandibular molar mesenchyme contained 87% and 65%, respectively, and the E14.0 *Msx1*$^{-/-}$ mutant maxillary and mandibular molar mesenchyme contained 88% and 64%, respectively, of the amount of *Bmp4* mRNAs present in the molar mesenchyme of littermate controls (Fig. 4). Thus, although the *Bmp4$^{f/f}$;Wnt1Cre* mutant embryos showed much more dramatic loss of *Bmp4* mRNAs in both maxillary and mandibular molar mesenchyme than did the *Msx1*$^{-/-}$ mutant embryos, the maxillary first molars in the *Bmp4$^{f/f}$;Wnt1Cre* mutant continued to develop to mineralized teeth but the corresponding maxillary first molars in the *Msx1*$^{-/-}$ mutant embryos were developmentally arrested at the bud stage. We verified further that the *Msx1*$^{-/-}$ mutant mouse tooth phenotype has not changed from previous studies: all nine late term *Msx1*$^{-/-}$ mutant mouse embryos examined showed bud stage arrest of both maxillary and mandibular molar tooth germs. These data indicate that the developmental arrest of the maxillary first molar tooth germs in the *Msx1*$^{-/-}$ mutant mice could not be due only to the decrease in mesenchymal *Bmp4* expression and suggest that normal bud-to-cap transition of molar tooth development requires at least one other Msx1-dependent odontogenic factor.

Msx1 expression is downregulated in the molar tooth mesenchyme and *Msx1* heterozygosity enhances maxillary molar developmental defects in *Bmp4$^{f/f}$;Wnt1Cre* mutant mice

Previous studies suggested that Bmp4 and Msx1 function in a positive-feedback loop to regulate the expression of each other in the developing tooth mesenchyme (Chen et al., 1996; Tucker et al., 1998; Vainio et al., 1993). We found that the levels of *Msx1* mRNA expression were consistently lower from E13.5 to E14.5 in both the maxillary and mandibular molar tooth mesenchyme in the *Bmp4$^{f/f}$;Wnt1Cre* mutant embryos in comparison with control littermates by using *in situ* hybridization analyses (Fig. 5A,B,D,E). Quantitative real-time RT-PCR analyses of LCM-isolated tooth mesenchyme samples showed that the levels of *Msx1* mRNAs were decreased by >50% in the mandibular molar mesenchyme in the *Bmp4$^{f/f}$;Wnt1Cre* mutant embryos by E14.5 in comparison with control littermates (Fig. 5C,F). By comparison, the reduction in *Msx1* mRNA expression in the maxillary molar tooth mesenchyme was not as dramatic as in the mandibular molar mesenchyme in the *Bmp4$^{f/f}$;Wnt1Cre* mutant embryos (Fig. 5C,F). To test whether the differences in *Msx1* expression levels could account for the distinct outcome of the maxillary and mandibular molar teeth, we examined tooth development in *Msx1*$^{+/-}$*Bmp4$^{f/-}$;Wnt1Cre* mutant mice. Whereas the *Bmp4$^{f/-}$;Wnt1Cre* mutant mice formed maxillary first and second molars that are reduced in size in comparison with their counterparts in the control littermates (Fig. 6A,B), the *Msx1*$^{+/-}$*Bmp4$^{f/-}$;Wnt1Cre* mutant mice formed only a much smaller maxillary first molar (Fig. 6C). Histological analyses of E18.5 embryos showed that the maxillary first molar tooth germs in the *Msx1*$^{+/-}$*Bmp4$^{f/-}$;Wnt1Cre* mutant embryos were dramatically smaller than the counterparts in the control and *Bmp4$^{f/-}$;Wnt1Cre* mutant embryos but still developed to the bell stage (Fig. 6D-F). By contrast, whereas the maxillary second molar tooth germs in the *Bmp4$^{f/-}$;Wnt1Cre* mutants were smaller than those in the control embryos (Fig. 6G,H), the second molar tooth germs failed to develop in the *Msx1*$^{+/-}$*Bmp4$^{f/-}$;Wnt1Cre* mutant embryos (Fig. 6I). These data indicate that the distinct maxillary and mandibular molar tooth phenotypes of the *Bmp4$^{f/f}$;Wnt1Cre* mutant mice could

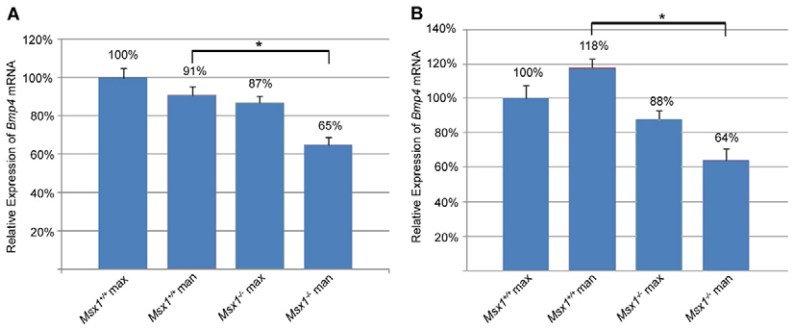

Fig. 4. Comparison of levels of *Bmp4* mRNAs in the maxillary and mandibular molar tooth mesenchyme in control and *Msx1*$^{-/-}$ mutant mouse embryos. (**A**) E13.5. (**B**) E14.0. Asterisk indicates significant difference between the sample pair (P<0.05). Error bars represent s.e.m.

not be explained simply by the differences in the levels of *Msx1* expression in the tooth mesenchyme but that the level of Msx1 expression is important for sequential molar tooth development.

The distinct maxillary and mandibular molar developmental defects in *Bmp4*$^{f/f}$*;Wnt1Cre* mutant mice correlate with differential gene expression profiles of the developing maxillary and mandibular molar tooth mesenchyme

To investigate the molecular basis of the dramatic difference in maxillary and mandibular molar tooth phenotypes in the *Bmp4*$^{f/f}$*;Wnt1Cre* mutant mice, we isolated maxillary and mandibular molar tooth mesenchyme from E13.5 *Bmp4*$^{f/f}$*;Wnt1Cre* mutant and wild-type littermates using LCM and carried out RNAseq analyses. Consistent with the real-time RT-PCR results (Fig. 1C), we found that the *Bmp4*$^{f/f}$*;Wnt1Cre* mutant maxillary and mandibular molar tooth mesenchyme contained <1% of wild-type levels of exon-4-containing *Bmp4* mRNAs and that the *Bmp4* mRNA levels were not significantly different between the maxillary and mandibular molar tooth mesenchyme in either the wild-type or the *Bmp4*$^{f/f}$*;Wnt1Cre* embryos (supplementary material Table S1).

We investigated whether other members of the Bmp family of ligands were differentially expressed in the developing maxillary and mandibular tooth mesenchyme. Of all Bmp family members other than Bmp4, only *Bmp3* and *Bmp6* mRNAs were detected at >5 reads per kilobase of transcript per million of mapped reads (RPKM) in maxillary and/or mandibular molar mesenchyme in the E13.5 wild-type embryos (supplementary material Table S2). These data are in agreement with previous *in situ* hybridization results showing expression of *Bmp3*, *Bmp4* and *Bmp6* mRNAs in the developing tooth mesenchyme whereas expression of *Bmp2* and *Bmp7* mRNAs was restricted to the tooth bud epithelium at E13.5 (Aberg et al., 1997). The RNAseq data show no significant differences in expression of other Bmp ligands that could account for the differences in maxillary and mandibular molar tooth defects in the *Bmp4*$^{f/f}$*;Wnt1Cre* mutant mice.

Analyses of the RNAseq data revealed that >170 genes are differentially expressed by more than twofold (P<0.01) in the wild-type maxillary versus mandibular molar tooth mesenchyme at E13.5. Among these, *Dkk2* transcripts were 3.5 times as abundant in the mandibular as in the maxillary molar mesenchyme (supplementary material Table S3). Transcripts for another Wnt antagonist, Wif1, were 2.4-fold as abundantly expressed in the mandibular as in the maxillary molar mesenchyme. Whereas *Wif1* expression levels were similar in the *Bmp4*$^{f/f}$*;Wnt1Cre* mutant and control molar tooth mesenchyme, *Dkk2* mRNA expression was significantly upregulated

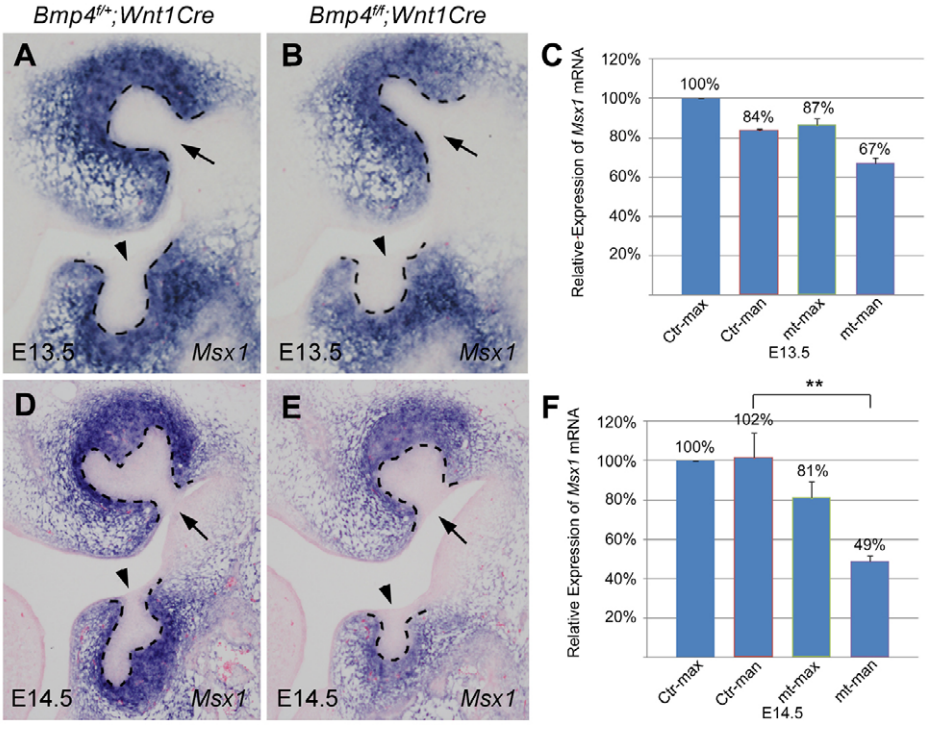

Fig. 5. Comparison of *Msx1* mRNA expression in developing tooth mesenchyme in control and *Bmp4*$^{f/f}$*;Wnt1Cre* mutant mouse embryos. (**A-C**) Comparison of *Msx1* mRNA expression in E13.5 control and *Bmp4*$^{f/f}$*;Wnt1Cre* mutant molar tooth mesenchyme by *in situ* hybridization (A,B) and real-time RT-PCR (C). Dashed lines mark the boundary between the dental epithelium and mesenchyme. Arrows point to maxillary first molar and arrowheads point to mandibular first molar tooth germ. (**D-F**) Comparison of *Msx1* mRNA expression in E14.5 control and *Bmp4*$^{f/f}$*;Wnt1Cre* mutant molar tooth mesenchyme by *in situ* hybridization (D,E) and real-time RT-PCR (F). The double asterisks in F indicate significant difference between the sample pair (P<0.01). Error bars represent s.e.m. Ctr-max, control maxillary; Ctr-Man, control mandibular; mt-max, mutant maxillary; mt-man, mutant mandibular.

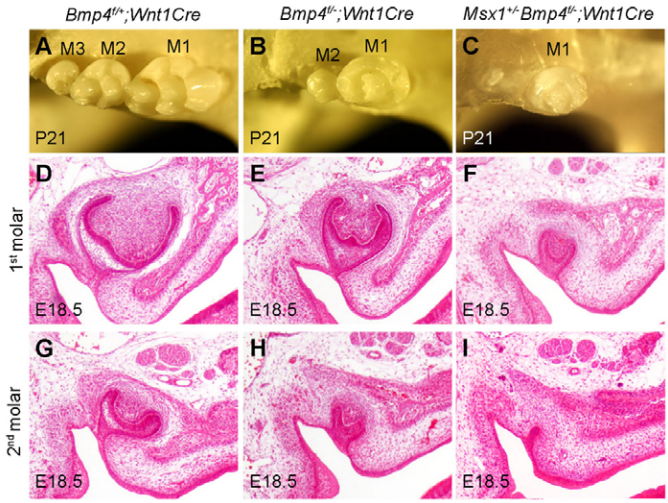

Fig. 6. Reducing *Msx1* gene dosage enhanced tooth developmental defects in *Bmp4$^{f/-}$;Wnt1Cre* mutant mice. (**A-C**) Skeletal preparations of P21 mice showing the maxillary molar regions. M1, M2 and M3 mark the first, second and third molars, respectively. (**D-F**) Hematoxylin and Eosin-stained frontal sections through the maxillary first molar tooth germs at E18.5. (**G-I**) Hematoxylin and Eosin-stained frontal sections through the maxillary second molar tooth germs at E18.5.

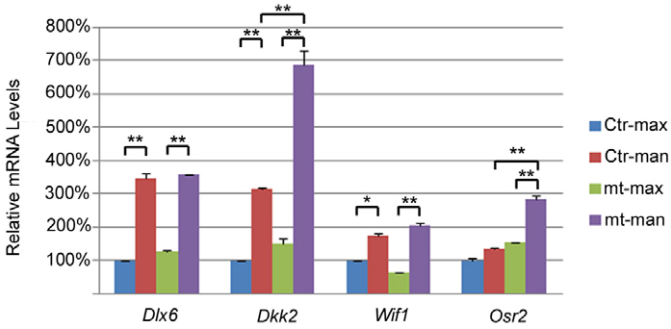

Fig. 7. Relative levels of expression of *Dlx6*, *Dkk2*, *Wif1* and *Osr2* mRNAs in the maxillary and mandibular molar mesenchyme in E13.5 control and *Bmp4$^{f/f}$;Wnt1Cre* mouse embryos. Error bars indicate s.e.m. *P<0.05, **P<0.01. Ctr-max, control maxillary; Ctr-Man, control mandibular; mt-max, mutant maxillary; mt-man, mutant mandibular.

in both the maxillary and mandibular molar mesenchyme in the *Bmp4$^{f/f}$;Wnt1Cre* mutant embryos in comparison with the wild-type embryos (supplementary material Table S3). These differences in *Dkk2* and *Wif1* mRNA levels between the maxillary and mandibular molar mesenchyme in the control and mutant embryos were verified further by using real-time RT-PCR analyses (Fig. 7). As Wnt signaling is crucial for the bud-to-cap transition during tooth development (Liu et al., 2008; Chen et al., 2009), the substantially higher levels of Dkk2 and Wif1 in the mandibular than maxillary molar mesenchyme could contribute to the more severe mandibular tooth defects in the *Bmp4$^{f/f}$;Wnt1Cre* mutant mice.

Osr2 expression was upregulated in molar tooth mesenchyme and genetic reduction of *Osr2* expression partially rescued mandibular molar development in *Bmp4$^{f/f}$;Wnt1Cre* mutant mice

We recently reported that the Osr2 transcription factor antagonizes Msx1-mediated propagation of mesenchymal odontogenic activity along the buccolingual axis to restrict molar tooth development in a single row (Zhang et al., 2009). Comparison of RNAseq data from the control and the *Bmp4$^{f/f}$;Wnt1Cre* mutant molar mesenchyme revealed that expression of *Osr2* mRNAs was increased in both the maxillary and mandibular molar tooth mesenchyme in the *Bmp4$^{f/f}$;Wnt1Cre* mutant embryos in comparison with the control samples (supplementary material Table S3). Both RNAseq and quantitative real-time RT-PCR analyses showed that *Osr2* mRNA expression was more significantly upregulated in the mandibular than in the maxillary molar mesenchyme such that *Osr2* mRNA levels were significantly more abundant in the mandibular than the maxillary molar mesenchyme in *Bmp4$^{f/f}$;Wnt1Cre* mutant embryos (Fig. 7; supplementary material Table S3). To investigate whether the increased *Osr2* expression contributed to the mandibular molar tooth developmental arrest in the *Bmp4$^{f/f}$;Wnt1Cre* mutant mice, we introduced the *Osr2* null mutation into the *Bmp4$^{f/f}$;Wnt1Cre* mice. We found that deleting one allele of *Osr2* partially rescued each mandibular first molar to a small mineralized tooth in the *Bmp4$^{f/f}$;Wnt1Cre* mutant mice (Fig. 8A-C). Examination of *Bmp4* mRNA expression in the developing molar tooth germs at E14.5 by *in situ* hybridization analyses showed that both *Bmp4$^{f/f}$;Wnt1Cre* and *Osr2$^{+/-}$Bmp4$^{f/f}$;Wnt1Cre* mutant embryos lack *Bmp4* expression in the tooth mesenchyme, but both maxillary and mandibular first molar tooth germs progressed to the cap stage and strongly expressed *Bmp4* mRNA in the PEK in the *Osr2$^{+/-}$Bmp4$^{f/f}$;Wnt1Cre* mutant embryos, in contrast to the bud stage arrest of the mandibular first molars in the *Bmp4$^{f/f}$;Wnt1Cre* mutant embryos (Fig. 8D-F). Real-time RT-PCR analyses of LCM-isolated maxillary and mandibular molar tooth mesenchyme confirmed that there was no restoration of *Bmp4* expression in the tooth mesenchyme in *Osr2$^{+/-}$Bmp4$^{f/f}$;Wnt1Cre* mutant embryos (supplementary material Fig. S4). Moreover, pSmad1/5 activation was similarly deficient in the developing molar tooth germs in *Bmp4$^{f/f}$;Wnt1Cre* and *Osr2$^{+/-}$Bmp4$^{f/f}$;Wnt1Cre* mutant embryos (Fig. 8G-I). However, both maxillary and mandibular molar tooth germs in the *Osr2$^{+/-}$Bmp4$^{f/-}$;Wnt1Cre* mutant embryos exhibited strong expression of *p21*, *Lef1* and *Fgf3* in the PEK at E14.5, similar to the *Bmp4$^{f/+}$;Wnt1Cre* control embryos and in contrast to the lack of PEK formation in the mandibular molar tooth germs in the *Bmp4$^{f/-}$;Wnt1Cre* mutant littermates (Fig. 9A-I). We further analyzed *Dkk2* expression in *Osr2$^{+/-}$Bmp4$^{f/f}$;Wnt1Cre* mutant embryos and found that *Dkk2* mRNA expression remained differentially expressed in the maxillary and mandibular mesenchyme and still significantly upregulated in both the maxillary and mandibular mesenchyme in comparison with control embryos (supplementary material Fig. S4). These data suggest that Bmp4 signaling plays an important role in the activation of mesenchymal odontogenic activity by suppressing the expression of tooth developmental antagonists, including Dkk2 and Osr2, in the developing tooth mesenchyme.

A crucial role for the Bmp4-Msx1 pathway in propagation of mesenchymal odontogenic activity during sequential molar tooth development

We previously showed that *Osr2$^{-/-}$* mutant mice develop supernumerary teeth from oral epithelium lingual to the molar teeth owing to expansion of the mesenchymal odontogenic field and that initiation of supernumerary tooth formation in the *Osr2$^{-/-}$* mice

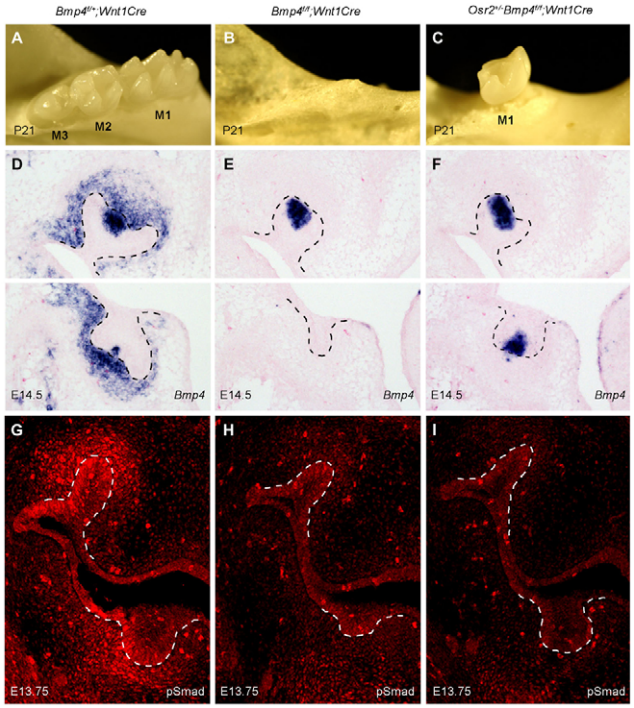

Fig. 8. *Osr2* heterozygosity partially rescued mandibular first molar development in *Bmp4$^{f/f}$;Wnt1Cre* mice. (**A-C**) Skeletal preparations showing P21 mandibular molar tooth region in control (A), *Bmp4$^{f/f}$;Wnt1Cre* (B) and *Osr2$^{+/-}$Bmp4$^{f/f}$;Wnt1Cre* (C) mice. M1, M2 and M3 mark the first, second and third molars, respectively. (**D-F**) *Bmp4* mRNA expression in the maxillary (upper) and mandibular (lower) first molar tooth germs in E14.5 control (D), *Bmp4$^{f/f}$;Wnt1Cre* (E) and *Osr2$^{+/-}$Bmp4$^{f/f}$;Wnt1Cre* (F) embryos. (**G-I**) pSmad1/5 immunofluorescent staining in the first molar tooth germs in the control (G), *Bmp4$^{f/f}$;Wnt1Cre* (H) and *Osr2$^{+/-}$Bmp4$^{f/f}$;Wnt1Cre* (I) embryos. Dashed lines mark boundary between dental epithelium and mesenchyme.

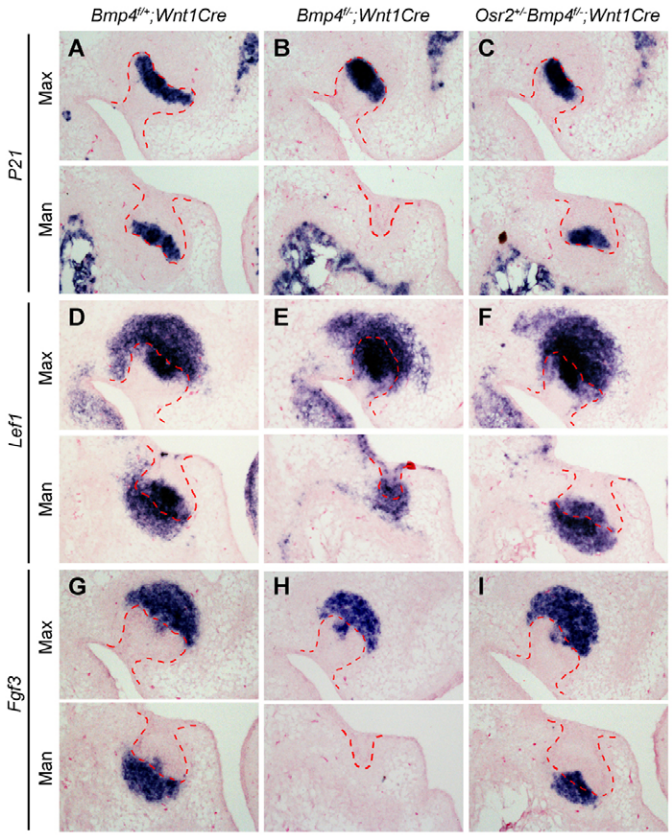

Fig. 9. Comparison of PEK molecular marker expression in control, *Bmp4$^{f/-}$;Wnt1Cre* and *Osr2$^{+/-}$Bmp4$^{f/-}$;Wnt1Cre* mutant mouse embryos at E14.5. (**A-C**) *P21* mRNA expression in the maxillary (Max) and mandibular (Man) first molar tooth germs. (**D-F**) *Lef1* mRNA expression. (**G-I**) *Fgf3* expression. Dashed lines mark boundary between dental epithelium and mesenchyme.

requires Msx1 function (Zhang et al., 2009). To investigate the role of mesenchymal Bmp4 in sequential tooth formation, we generated and analyzed molar tooth development in *Osr2$^{-/-}$Bmp4$^{f/f}$;Wnt1Cre* mutant mice. Histological analyses of newborn *Osr2$^{-/-}$Bmp4$^{f/f}$;Wnt1Cre* mutant mice did not detect supernumerary tooth germs lingual to their molars, although all *Osr2$^{-/-}$* mutant littermates showed supernumerary teeth (Fig. 10A,B). We then analyzed the mutant embryos at E15.5 to investigate whether the *Osr2$^{-/-}$Bmp4$^{f/f}$;Wnt1Cre* mutant embryos failed to initiate supernumerary tooth formation. An area of aberrantly thickened oral epithelium expressing the tooth epithelial marker *Pitx2* was clearly observed lingual to each of the mandibular first molar tooth germs in the *Osr2$^{-/-}$Bmp4$^{f/f}$;Wnt1Cre* mutant embryos, similar to observations in the *Osr2$^{-/-}$* mutant littermates (Fig. 10C-F), indicating that supernumerary tooth development was initiated in the *Osr2$^{-/-}$Bmp4$^{f/f}$;Wnt1Cre* mutant embryos. However, in contrast to the expansion of *Msx1* mRNA expression to the mesenchyme underlying the supernumerary tooth placode in the *Osr2$^{-/-}$* mutant embryos, *Msx1* mRNA expression was significantly reduced in the mandibular fist molar tooth mesenchyme and did not expand to the mesenchyme underlying the supernumerary tooth placode in the *Osr2$^{-/-}$Bmp4$^{f/f}$;Wnt1Cre* mutant embryos (Fig. 10G,H). The lack of expansion of *Msx1* expression to the mesenchyme underlying the supernumerary tooth placode accounts for the subsequent failure of supernumerary tooth morphogenesis in the *Osr2$^{-/-}$Bmp4$^{f/f}$;Wnt1Cre* mutant mice and indicates that mesenchymal Bmp4 signaling is required to propagate *Msx1* expression during sequential tooth formation.

In addition to lack of supernumerary tooth initiation, the *Msx1$^{-/-}$Osr2$^{-/-}$* double mutant mice did not develop second molars although their first molars developed beyond the bell stage and there was clearly detected *Bmp4* expression in the developing molar tooth mesenchyme (Zhang et al., 2009). By contrast, we consistently detected a small second molar tooth germ that had progressed to the cap stage in addition to a late bell stage first molar tooth germ in each half of the mandible in P0 *Osr2$^{-/-}$Bmp4$^{f/f}$;Wnt1Cre* mutant mice (Fig. 11; supplementary material Fig. S5). As the *Msx1$^{-/-}$Osr2$^{-/-}$* mutant embryos showed clearly detectable *Bmp4* mRNA expression in the molar tooth mesenchyme (Zhang et al., 2009), the formation of supernumerary and second molar tooth germs in the *Osr2$^{-/-}$Bmp4$^{f/f}$;Wnt1Cre* mutant but not in *Msx1$^{-/-}$Osr2$^{-/-}$* mutant embryos indicate that other Msx1-dependent odontogenic factors in addition to Bmp4 are required for the induction of sequential molar tooth formation.

DISCUSSION

Because the bud stage tooth developmental arrest in *Msx1$^{-/-}$* mutant mice was associated with a reduction in *Bmp4* mRNA

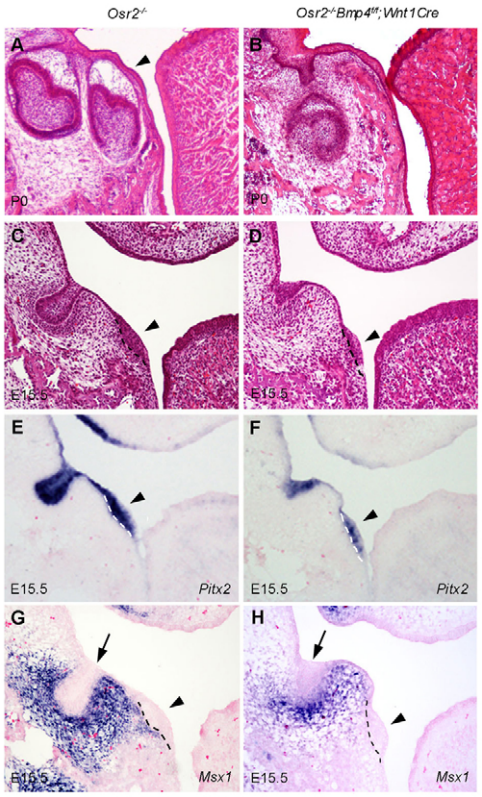

Fig. 10. *Osr2*$^{-/-}$*Bmp4*$^{f/f}$*;Wnt1Cre* double mutant mice showed initiation and subsequent arrest of supernumerary tooth germs. (**A-D**) Hematoxylin and Eosin-stained frontal sections through the posterior region of mandibular first molar tooth germs in *Osr2*$^{-/-}$ (A,C) and *Osr2*$^{-/-}$*Bmp4*$^{f/f}$*;Wnt-Cre* (B,D) embryos at P0 (A,B) and E15.5 (C,D). Arrowheads point to the supernumerary tooth germ. (**E**,**F**) Expression of *Pitx2* mRNAs in the tooth germs in E15.5 *Osr2*$^{-/-}$ (E) and *Osr2*$^{-/-}$*Bmp4*$^{f/f}$*;Wnt1Cre* (F) embryos. Dashed line marks boundary between the supernumerary dental placode epithelium and mesenchyme. (**G**,**H**) Expression of *Msx1* mRNAs in the tooth mesenchyme in E15.5 *Osr2*$^{-/-}$ (G) and *Osr2*$^{-/-}$*Bmp4*$^{f/f}$*;Wnt1Cre* (H) embryos. Arrows point to the first molar tooth germ and arrowheads point to the supernumerary tooth germ. Dashed lines mark the boundary between epithelium and mesenchyme of the developing supernumerary tooth germs.

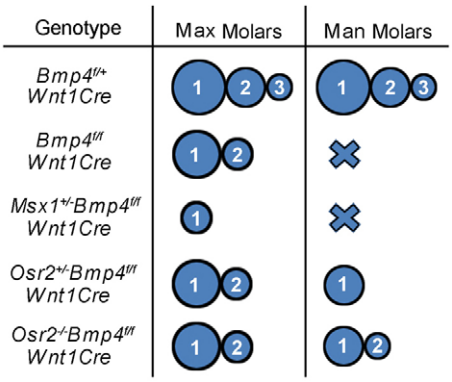

Fig. 11. Summary of the effects of *Bmp4*, *Msx1* and *Osr2* mutations on sequential molar development. Each row shows the schematic representation of the molar tooth patterns in a maxillary (Max) and a mandibular (Man) quadrant for the indicated genotype. Cross indicates tooth developmental arrest at the bud stage.

expression in the tooth mesenchyme and addition of exogenous Bmp4 protein or transgenic overexpression of Bmp4 was able to partially rescue *Msx1*$^{-/-}$ mutant mandibular molar tooth germs through the bud-to-cap transition, it has been concluded that mesenchymal Bmp4 is responsible for and required for driving molar tooth morphogenesis through the bud-to-cap transition (Chen et al., 1996; Bei et al., 2000; Zhao et al., 2000). This conclusion has been widely accepted and applied as an established principle for interpreting tooth developmental phenotypes, although the role of endogenous mesenchymal Bmp4 in tooth development has not been previously directly investigated. For example, a 24-hour stalling of the molar tooth buds from E13.5 to E14.5 in *Barx1*$^{-/-}$ mutant embryos was suggested to be caused by a reduction of mesenchymal *Bmp4* mRNA expression in the tooth mesenchyme at E13.5 as detected by *in situ* hybridization (Miletich et al., 2011). Miletich et al. further hypothesized that the subsequent resumption of molar tooth morphogenesis in the *Barx1*$^{-/-}$ mice, following the bud stage stalling, was due to mesenchymal Bmp accumulating and reaching an optimal level by E14.5 (Miletich et al., 2011). In this study, we have directly investigated the role of endogenous mesenchymal Bmp4 in tooth development. We found that maxillary first molar tooth germs in the *Bmp4*$^{f/f}$*;Wnt1Cre* mutant mice developed through the bud-to-cap transition in pace with those in the control littermates although the *Bmp4* gene was irreversibly inactivated in the cranial neural crest cells and the residual level of *Bmp4* mRNA in *Bmp4*$^{f/f}$*;Wnt1Cre* maxillary molar tooth mesenchyme was much lower than that in *Msx1*$^{-/-}$ maxillary molar tooth mesenchyme. These data indicate that at least the maxillary molar tooth bud arrest in *Msx1*$^{-/-}$ mutant mice was not solely due to the reduction in mesenchymal *Bmp4* expression. Moreover, as there was clearly detected *Bmp4* mRNA expression in the molar tooth bud mesenchyme in *Barx1*$^{-/-}$ mutant embryos at E13.5 (Miletich et al., 2011), in contrast to undetectable *Bmp4* mRNA expression in the *Bmp4*$^{f/f}$*;Wnt1Cre* maxillary molar mesenchyme by *in situ* hybridization, the molecular mechanism underlying bud stage stalling of molar tooth germs in *Barx1*$^{-/-}$ mutant mice is likely to involve other Barx1-regulated factors in addition to Bmp4, which warrants further investigation.

If the molar tooth developmental arrest in *Msx1*$^{-/-}$ mutant mice was not solely due to decreased *Bmp4* expression, why was exogenous Bmp4 protein or transgenic *Bmp4* overexpression able to rescue morphogenesis of the *Msx1*$^{-/-}$ mutant molar tooth germs (Bei et al., 2000; Zhao et al., 2000)? We previously demonstrated that *Msx1*$^{-/-}$*Osr2*$^{-/-}$ double homozygous mutant mice exhibited first molar morphogenesis to the bell stage (Zhang et al., 2009), indicating that Msx1 and Osr2 act antagonistically to regulate mesenchymal odontogenic activity but at least one other endogenous factor could activate mesenchymal odontogenic activity in the absence of both Msx1 and Osr2. In this study, we found that expression of *Osr2* was significantly upregulated in the *Bmp4*$^{f/f}$*;Wnt1Cre* mutant molar mesenchyme and that reduction of *Osr2* gene dosage partially rescued *Bmp4*$^{f/f}$*;Wnt1Cre* mutant mandibular molar morphogenesis without restoring mesenchymal *Bmp4* expression. Thus, it is possible that the exogenous or overexpressed Bmp4 was able to restore odontogenic activity of the *Msx1*$^{-/-}$ mutant molar mesenchyme through downregulation of Osr2 and/or activation of other odontogenic activators. In addition, other factors in the fetal calf serum or chick embryo extract used in the explant culture medium might have acted synergistically with exogenous Bmp4 protein as a high percentage of the *Msx1*$^{-/-}$

tooth germ explants supplemented with exogenous Bmp4 progressed to the stage of dentin formation whereas the *Bmp4* transgene driven by the *Msx1* promoter only rescued a low percentage of *Msx1*$^{-/-}$ mutant molar tooth germs to early cap stage without further morphogenesis (Bei et al., 2000; Zhao et al., 2000). Thus, although our findings indicate that endogenous mesenchymal Bmp4 plays crucial roles in tooth development, this study reveals an important gap in the understanding of Msx1-mediated regulation of mesenchymal odontogenic activity. Moreover, our data indicate an essential role for Bmp4 signaling in the regulation of mesenchymal odontogenic activity through suppression of *Osr2* expression and in modulation of Wnt signaling during tooth development through suppression of *Dkk2* expression.

Previous studies of *Inhba*$^{-/-}$ and *Dlx1/2*$^{-/-}$ mutant mice have suggested that development of the maxillary and mandibular molar teeth might involve distinct molecular pathways (Ferguson et al., 1998; Thomas et al., 1997). In particular, maxillary molar tooth development, uniquely, does not require activin signaling although expression of genes downstream of activin signaling, including follistatin and *Irx1*, were downregulated in both the maxillary and mandibular molar tooth germs in the *Inhba*$^{-/-}$ mutant embryos (Ferguson et al., 1998; Ferguson et al., 2000). Similarly, we found that the *Bmp4*$^{f/f}$*;Wnt1Cre* mutant embryos exhibited loss of pSmad1/5 as well as dental epithelial expression of *Dlx2* in both maxillary and mandibular molar tooth germs, although only the mandibular molar tooth germs were arrested at the bud stage. Our RNAseq analysis revealed that the wild-type maxillary and mandibular molar mesenchyme exhibit significantly different gene expression profiles, which is consistent with the hypothesis that maxillary and mandibular molar development employ distinct molecular pathways. However, we found that two secreted Wnt antagonists, Dkk2 and Wif1, are expressed at much higher levels in the mandibular than maxillary molar mesenchyme. Wnt signaling is required in both the epithelium and mesenchyme for either maxillary or mandibular tooth development to progress beyond the bud stage (Chen et al., 2009; Liu et al., 2008). Thus, it is likely that mandibular molar tooth development requires higher levels of mesenchymal odontogenic activity than the maxillary molar germs to overcome the significantly higher levels of Wnt antagonists. In the *Bmp4*$^{f/f}$*;Wnt1Cre* mutant embryos, expression of *Dkk2* and *Osr2* are further increased in the mandibular molar mesenchyme. Genetic reduction of *Osr2* gene dosage by 50% in *Bmp4*$^{f/f}$*;Wnt1Cre* mutant embryos was able to rescue the mandibular first molar tooth development through the bud-to-cap transition. As Osr2 is known to antagonize Msx1-mediated activation of mesenchymal odontogenic activity (Zhang et al., 2009), and mesenchymal *Bmp4* expression was not restored in the *Osr2*$^{+/-}$ *Bmp4*$^{f/f}$*;Wnt1Cre* mutant embryos, a logical explanation is that reducing *Osr2* expression allowed sufficient activation of other odontogenic signals by Msx1 to drive the mandibular first molar tooth germs through the bud-to-cap transition in these embryos. Thus, although maxillary and mandibular molar tooth germs exhibit distinct gene expression profiles, the distinct phenotypes of maxillary versus mandibular molar tooth development in *Bmp4*$^{f/f}$*;Wnt1Cre* mutant embryos appear to be due to the mandibular molar mesenchyme expressing higher levels of antagonists of the common odontogenic pathways than the maxillary molar mesenchyme. Further analysis of the molecular mechanisms underlying the differences in maxillary and mandibular molar tooth phenotypes in the *Inhba*$^{-/-}$ mutant mice is necessary to clarify this issue.

Using tooth germ explant cultures, Kavanagh et al. (Kavanagh et al., 2007) showed that mouse mandibular first molar tooth germ inhibited second molar tooth development and they proposed an inhibitory cascade model, in which initiation of the posterior molar depended on a balance between intermolar inhibition and mesenchymal activation. Similar activator-inhibitor mechanisms have been proposed for periodic dentition patterning in other vertebrates (Smith, 2003; Streelman et al., 2003). However, the molecular mechanisms controlling sequential tooth initiation have not been elucidated. In this study, we found that the *Bmp4*$^{f/f}$*;Wnt1Cre* mutant mice developed mineralized maxillary first and second molars but lacked the third molar. Reducing the *Msx1* gene dosage by 50% in the *Bmp4*$^{f/f}$*;Wnt1Cre* mutant background blocked maxillary second molar development. By contrast, reducing the *Osr2* gene dosage by 50% partially rescued mandibular first molar development and complete knockout of *Osr2* also partially rescued mandibular second molar development in the *Bmp4*$^{f/f}$*;Wnt1Cre* mutant mice (Fig. 11). Whereas the downregulation of *Msx1* expression in the first molar mesenchyme and lack of expansion of *Msx1* expression into the supernumerary tooth mesenchyme in the *Osr2*$^{-/-}$ *Bmp4*$^{f/f}$*;Wnt1Cre* mutant embryos support a crucial role of the Bmp4-Msx1 positive feedback loop for propagation of Msx1 and Bmp4 expression during sequential tooth development, the findings that both supernumerary tooth germ and second molar development were initiated in the *Osr2*$^{-/-}$ *Bmp4*$^{f/f}$*;Wnt1Cre* mutant embryos but not in *Msx1*$^{-/-}$ *Osr2*$^{-/-}$ mutant embryos, which had clearly detectable *Bmp4* expression in the molar mesenchyme (Zhang et al., 2009), indicate that other Msx1-dependent mesenchymal odontogenic activity, in addition to Bmp4, is required for sequential tooth development. Taken together, these data indicate that Bmp4 and Msx1 positively regulate each other's expression in the developing tooth mesenchyme and that Msx1 activates other mesenchymal odontogenic factors in addition to Bmp4 to drive tooth morphogenesis through the bud-to-cap transition as well as to induce sequential tooth formation.

Acknowledgements
We thank Steven Potter and Eric Brunskill for technical advice on laser capture microdissection and RNAseq data analyses. We thank the Gene Expression Microarray Core and the Genetic Variation and Gene Discovery Core facilities at Cincinnati Children's Hospital Medical Center for RNA quality analysis, cDNA amplification, and next-generation sequencing services.

Funding
This work was supported by the National Institutes of Health (NIH) National Institute of Dental and Craniofacial Research (NIDCR) [grants DE018401, DE013681 and DE015207 to R.J. and DE012324 to J.F.M.]. Deposited in PMC for release after 12 months.

Competing interests statement
The authors declare no competing financial interests.

Supplementary material
Supplementary material available online at
http://dev.biologists.org/lookup/suppl/doi:10.1242/dev.081927/-/DC1

References

Aberg, T., Wozney, J. and Thesleff, I. (1997). Expression patterns of bone morphogenetic proteins (Bmps) in the developing mouse tooth suggest roles in morphogenesis and cell differentiation. *Dev. Dyn.* **210**, 383-396.
Andl, T., Ahn, K., Kairo, A., Chu, E. Y., Wine-Lee, L., Reddy, S. T., Croft, N. J., Cebra-Thomas, J. A., Metzger, D., Chambon, P. et al. (2004). Epithelial Bmpr1a regulates differentiation and proliferation in postnatal hair follicles and is essential for tooth development. *Development* **131**, 2257-2268.
Bei, M., Kratochwil, K. and Maas, R. L. (2000). BMP4 rescues a non-cell-autonomous function of Msx1 in tooth development. *Development* **127**, 4711-4718.
Brunskill, E. W. and Potter, S. S. (2012). RNA-Seq defines novel genes, RNA processing patterns and enhancer maps for the early stages of nephrogenesis: Hox supergenes. *Dev. Biol.* **368**, 4-17.

Chai, Y., Jiang, X., Ito, Y., Bringas, P., Jr, Han, J., Rowitch, D. H., Soriano, P., McMahon, A. P. and Sucov, H. M. (2000). Fate of the mammalian cranial neural crest during tooth and mandibular morphogenesis. *Development* **127**, 1671-1679.
Chen, Y., Bei, M., Woo, I., Satokata, I. and Maas, R. (1996). Msx1 controls inductive signaling in mammalian tooth morphogenesis. *Development* **122**, 3035-3044.
Chen, J., Lan, Y., Baek, J. A., Gao, Y. and Jiang, R. (2009). Wnt/beta-catenin signaling plays an essential role in activation of odontogenic mesenchyme during early tooth development. *Dev. Biol.* **334**, 174-185.
Danielian, P. S., Muccino, D., Rowitch, D. H., Michael, S. K. and McMahon, A. P. (1998). Modification of gene activity in mouse embryos in utero by a tamoxifen-inducible form of Cre recombinase. *Curr. Biol.* **8**, 1323-1326.
Ferguson, C. A., Tucker, A. S., Christensen, L., Lau, A. L., Matzuk, M. M. and Sharpe, P. T. (1998). Activin is an essential early mesenchymal signal in tooth development that is required for patterning of the murine dentition. *Genes Dev.* **12**, 2636-2649.
Ferguson, C. A., Tucker, A. S. and Sharpe, P. T. (2000). Temporospatial cell interactions regulating mandibular and maxillary arch patterning. *Development* **127**, 403-412.
Han, J., Ito, Y., Yeo, J. Y., Sucov, H. M., Maas, R. and Chai, Y. (2003). Cranial neural crest-derived mesenchymal proliferation is regulated by Msx1-mediated p19(INK4d) expression during odontogenesis. *Dev. Biol.* **261**, 183-196.
Hefti, E., Trechsel, U., Rüfenacht, H. and Fleisch, H. (1980). Use of dermestid beetles for cleaning bones. *Calcif. Tissue Int.* **31**, 45-47.
Jernvall, J. and Thesleff, I. (2000). Reiterative signaling and patterning during mammalian tooth morphogenesis. *Mech. Dev.* **92**, 19-29.
Jernvall, J., Aberg, T., Kettunen, P., Keränen, S. and Thesleff, I. (1998). The life history of an embryonic signaling center: BMP-4 induces p21 and is associated with apoptosis in the mouse tooth enamel knot. *Development* **125**, 161-169.
Kavanagh, K. D., Evans, A. R. and Jernvall, J. (2007). Predicting evolutionary patterns of mammalian teeth from development. *Nature* **449**, 427-432.
Kollar, E. J. and Baird, G. R. (1970). Tissue interactions in embryonic mouse tooth germs. II. The inductive role of the dental papilla. *J. Embryol. Exp. Morphol.* **24**, 173-186.
Kollar, E. J. and Fisher, C. (1980). Tooth induction in chick epithelium: expression of quiescent genes for enamel synthesis. *Science* **207**, 993-995.
Lan, Y., Ovitt, C. E., Cho, E. S., Maltby, K. M., Wang, Q. and Jiang, R. (2004). Odd-skipped related 2 (Osr2) encodes a key intrinsic regulator of secondary palate growth and morphogenesis. *Development* **131**, 3207-3216.
Liu, W., Sun, X., Braut, A., Mishina, Y., Behringer, R. R., Mina, M. and Martin, J. F. (2005). Distinct functions for Bmp signaling in lip and palate fusion in mice. *Development* **132**, 1453-1461.
Liu, F., Chu, E. Y., Watt, B., Zhang, Y., Gallant, N. M., Andl, T., Yang, S. H., Lu, M. M., Piccolo, S., Schmidt-Ullrich, R. et al. (2008). Wnt/beta-catenin signaling directs multiple stages of tooth morphogenesis. *Dev. Biol.* **313**, 210-224.
Lumsden, A. G. (1988). Spatial organization of the epithelium and the role of neural crest cells in the initiation of the mammalian tooth germ. *Development* **103**, 155-169.
Miletich, I., Yu, W. Y., Zhang, R., Yang, K., Caixeta de Andrade, S., Pereira, S. F., Ohazama, A., Mock, O. B., Buchner, G., Sealby, J. et al. (2011). Developmental stalling and organ-autonomous regulation of morphogenesis. *Proc. Natl. Acad. Sci. USA* **108**, 19270-19275.
Mina, M. and Kollar, E. J. (1987). The induction of odontogenesis in non-dental mesenchyme combined with early murine mandibular arch epithelium. *Arch. Oral Biol.* **32**, 123-127.
Mostowska, A., Biedziak, B. and Jagodzinski, P. P. (2012). Novel MSX1 mutation in a family with autosomal-dominant hypodontia of second premolars and third molars. *Arch. Oral Biol.* **57**, 790-795.
Nakatomi, M., Wang, X. P., Key, D., Lund, J. J., Turbe-Doan, A., Kist, R., Aw, A., Chen, Y., Maas, R. L. and Peters, H. (2010). Genetic interactions between Pax9 and Msx1 regulate lip development and several stages of tooth morphogenesis. *Dev. Biol.* **340**, 438-449.
O'Connell, D. J., Ho, J. W., Mammoto, T., Turbe-Doan, A., O'Connell, J. T., Haseley, P. S., Koo, S., Kamiya, N., Ingber, D. E., Park, P. J. et al. (2012). A Wnt-bmp feedback circuit controls intertissue signaling dynamics in tooth organogenesis. *Sci. Signal.* **5**, ra4.
Ogawa, T., Kapadia, H., Feng, J. Q., Raghow, R., Peters, H. and D'Souza, R. N. (2006). Functional consequences of interactions between Pax9 and Msx1 genes in normal and abnormal tooth development. *J. Biol. Chem.* **281**, 18363-18369.
Peters, H., Neubüser, A., Kratochwil, K. and Balling, R. (1998). Pax9-deficient mice lack pharyngeal pouch derivatives and teeth and exhibit craniofacial and limb abnormalities. *Genes Dev.* **12**, 2735-2747.
Ruch, J. V., Karcher-Djuricic, V. and Gerber, R. (1973). Determinants of morphogénesis and cytodifferentiations of dental anloges in mice. *J. Biol. Buccale* **1**, 45-56.
Satokata, I. and Maas, R. (1994). Msx1 deficient mice exhibit cleft palate and abnormalities of craniofacial and tooth development. *Nat. Genet.* **6**, 348-356.
Smith, M. M. (2003). Vertebrate dentitions at the origin of jaws: when and how pattern evolved. *Evol. Dev.* **5**, 394-413.
Stockton, D. W., Das, P., Goldenberg, M., D'Souza, R. N. and Patel, P. I. (2000). Mutation of PAX9 is associated with oligodontia. *Nat. Genet.* **24**, 18-19.
Streelman, J. T., Webb, J. F., Albertson, R. C. and Kocher, T. D. (2003). The cusp of evolution and development: a model of cichlid tooth shape diversity. *Evol. Dev.* **5**, 600-608.
Thomas, B. L., Tucker, A. S., Qui, M., Ferguson, C. A., Hardcastle, Z., Rubenstein, J. L. and Sharpe, P. T. (1997). Role of Dlx-1 and Dlx-2 genes in patterning of the murine dentition. *Development* **124**, 4811-4818.
Tucker, A. and Sharpe, P. (2004). The cutting-edge of mammalian development; how the embryo makes teeth. *Nat. Rev. Genet.* **5**, 499-508.
Tucker, A. S., Al Khamis, A. and Sharpe, P. T. (1998). Interactions between Bmp-4 and Msx-1 act to restrict gene expression to odontogenic mesenchyme. *Dev. Dyn.* **212**, 533-539.
Vainio, S., Karavanova, I., Jowett, A. and Thesleff, I. (1993). Identification of BMP-4 as a signal mediating secondary induction between epithelial and mesenchymal tissues during early tooth development. *Cell* **75**, 45-58.
Vastardis, H., Karimbux, N., Guthua, S. W., Seidman, J. G. and Seidman, C. E. (1996). A human MSX1 homeodomain missense mutation causes selective tooth agenesis. *Nat. Genet.* **13**, 417-421.
Winnier, G., Blessing, M., Labosky, P. A. and Hogan, B. L. (1995). Bone morphogenetic protein-4 is required for mesoderm formation and patterning in the mouse. *Genes Dev.* **9**, 2105-2116.
Zhang, Y., Zhao, X., Hu, Y., St Amand, T., Zhang, M., Ramamurthy, R., Qiu, M. and Chen, Y. (1999). Msx1 is required for the induction of Patched by Sonic hedgehog in the mammalian tooth germ. *Dev. Dyn.* **215**, 45-53.
Zhang, Z., Song, Y., Zhao, X., Zhang, X., Fermin, C. and Chen, Y. (2002). Rescue of cleft palate in Msx1-deficient mice by transgenic Bmp4 reveals a network of BMP and Shh signaling in the regulation of mammalian palatogenesis. *Development* **129**, 4135-4146.
Zhang, Y. D., Chen, Z., Song, Y. Q., Liu, C. and Chen, Y. P. (2005). Making a tooth: growth factors, transcription factors, and stem cells. *Cell Res.* **15**, 301-316.
Zhang, Z., Lan, Y., Chai, Y. and Jiang, R. (2009). Antagonistic actions of Msx1 and Osr2 pattern mammalian teeth into a single row. *Science* **323**, 1232-1234.
Zhao, X., Zhang, Z., Song, Y., Zhang, X., Zhang, Y., Hu, Y., Fromm, S. H. and Chen, Y. (2000). Transgenically ectopic expression of Bmp4 to the Msx1 mutant dental mesenchyme restores downstream gene expression but represses Shh and Bmp2 in the enamel knot of wild type tooth germ. *Mech. Dev.* **99**, 29-38.
Zhou, J., Gao, Y., Zhang, Z., Zhang, Y., Maltby, K. M., Liu, Z., Lan, Y. and Jiang, R. (2011). Osr2 acts downstream of Pax9 and interacts with both Msx1 and Pax9 to pattern the tooth developmental field. *Dev. Biol.* **353**, 344-353.

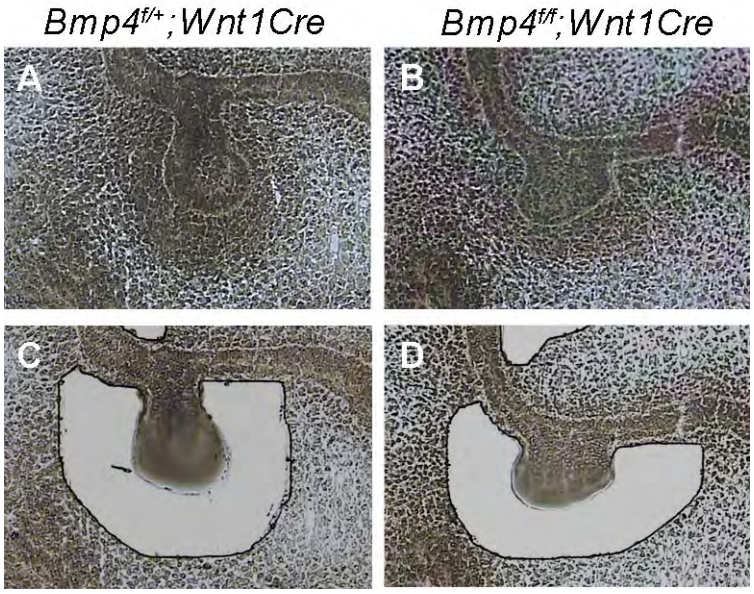

Fig. S1. Representative images of sections of E13.5 first molar tooth germs before and after LCM isolation of tooth mesenchyme. (**A**,**C**) *Bmp4$^{f/+}$;Wnt1Cre* control samples. (**B**,**D**) *Bmp4$^{f/f}$;Wnt1Cre* mutant samples.

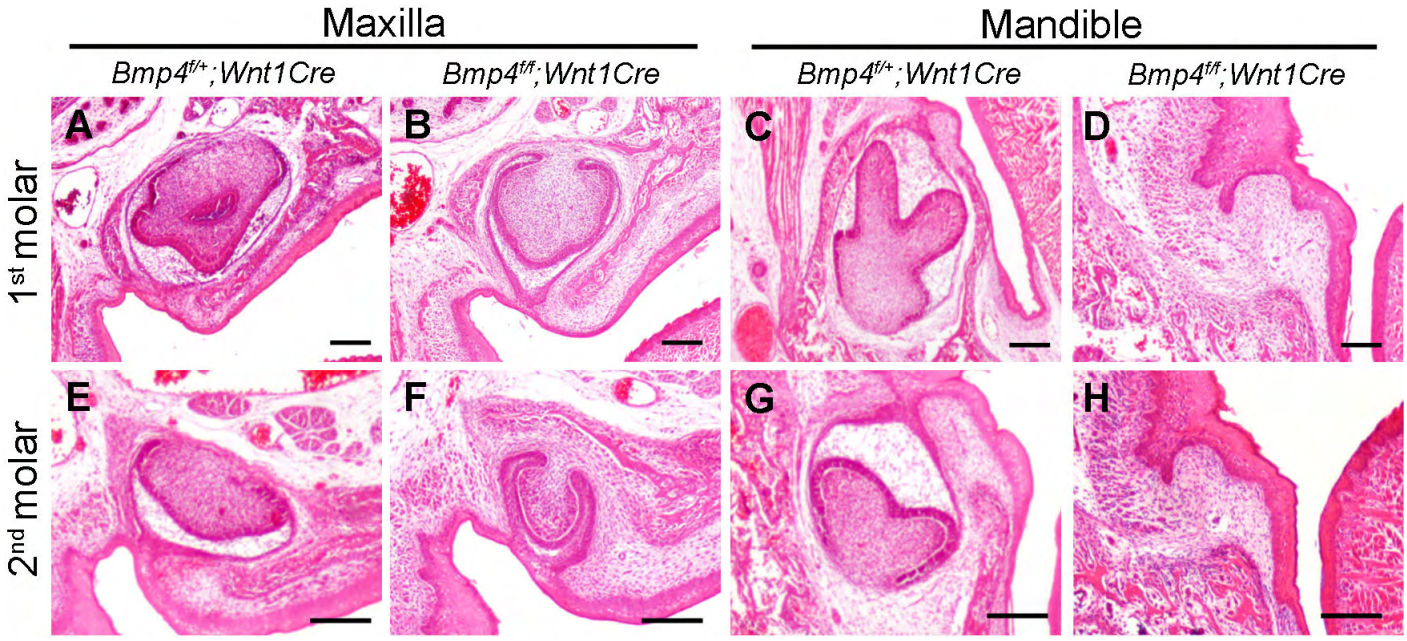

Fig. S2. *Bmp4$^{f/f}$Wnt1Cre* mutant mice exhibit developmental arrest of mandibular molar and delayed development of maxillary molar tooth germs. (**A-D**) Hematoxylin and Eosin-stained frontal sections through the first molar tooth germs of P0 control and mutant mice. (**E-H**) Hematoxylin and Eosin-stained frontal sections through the second molar tooth germs of control and mutant mice. Scale bars: 50 μm.

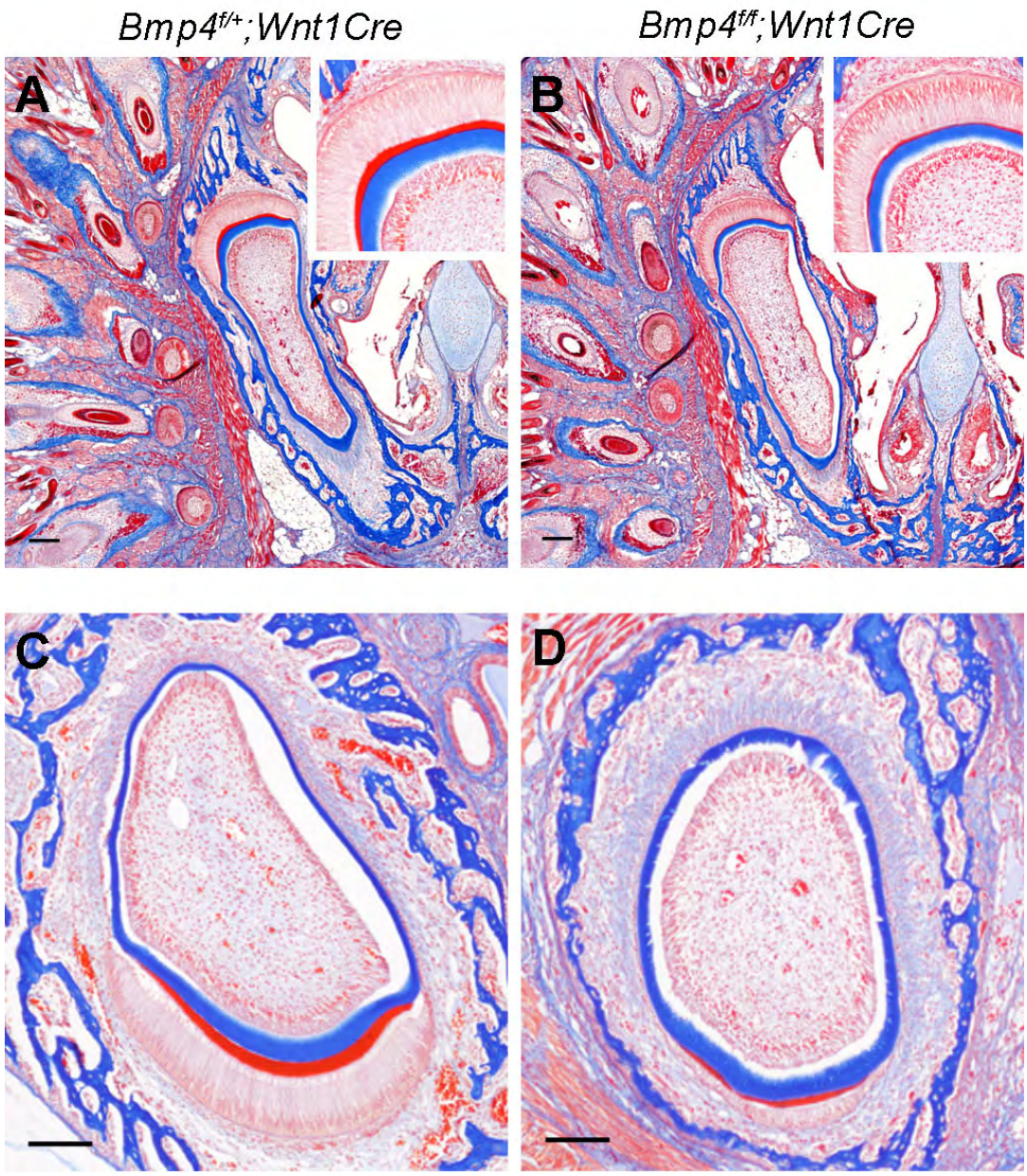

Fig. S3. Histological analyses of incisor defects in the *Bmp4$^{f/f}$;Wnt1Cre* mutant mice. Frontal sections of P5 mice were assayed by trichrome staining. The enamel matrix was stained red and dentin matrix blue. (**A**,**B**) The upper incisors. The inset at the upper-right corner of the panel shows higher magnification view of the ameloblast and odontoblast layers at the labile side of the tooth germ. (**C**,**D**) The lower incisors. The mutant lower incisor (D) was more rounded and had thinner enamel layer on the labile surface than that in the control littermate (C). Scale bars: 100 μm.

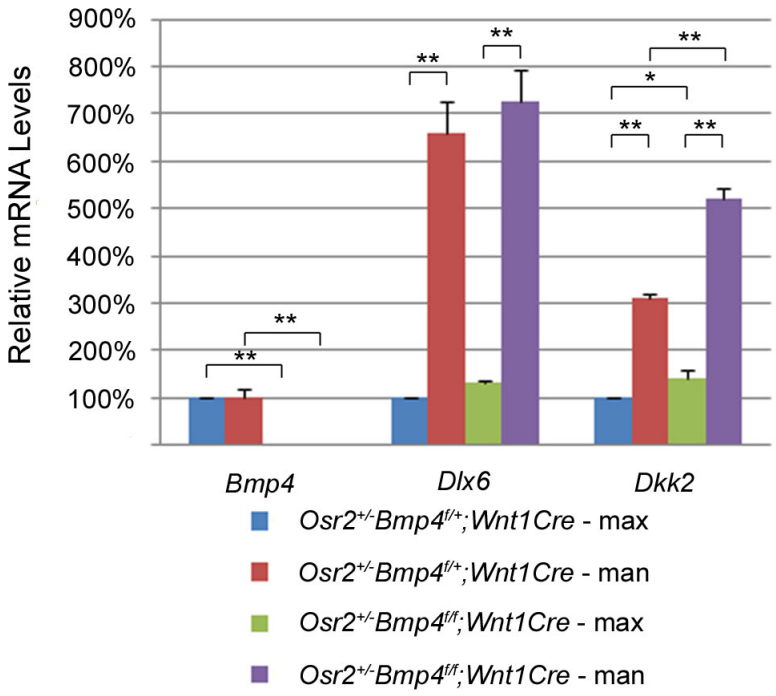

Fig. S4. Relative levels of *Bmp4*, *Dlx6* and *Dkk2* mRNAs, respectively, in the maxillary and mandibular molar mesenchyme in control and *Osr2*$^{+/-}$*Bmp4*$^{f/f}$*;Wnt1Cre* mutant embryos. **P*<0.05, ***P*<0.01.

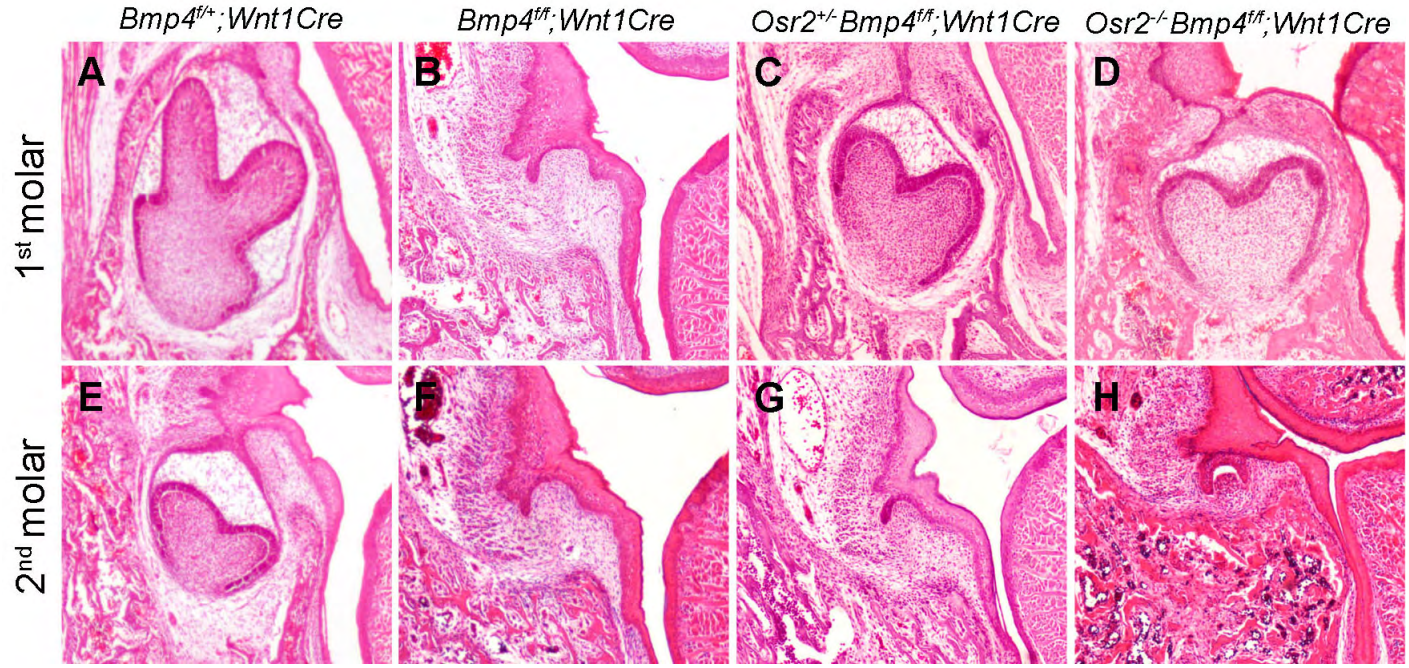

Fig. S5. Mandibular molar development in the *Osr2*$^{-/-}$*Bmp4*$^{f/-}$*;Wnt1Cre* compound mutant mice. (**A-D**) Hematoxylin and Eosin-stained frontal sections through the developing mandibular first molar tooth germs of *Bmp4*$^{f/+}$*;Wnt1Cre* (A), *Bmp4*$^{f/f}$*;Wnt1Cre* (B), *Osr2*$^{+/-}$*Bmp4*$^{f/-}$*;Wnt1Cre* (C) and *Osr2*$^{-/-}$*Bmp4*$^{f/-}$*;Wnt1Cre* (D) mutant pups at P0. (**E-H**) Hematoxylin and Eosin-stained frontal sections through the developing mandibular second molar tooth germs of *Bmp4*$^{f/+}$*;Wnt1Cre* (E), *Bmp4*$^{f/f}$*;Wnt1Cre* (F), *Osr2*$^{+/-}$*Bmp4*$^{f/-}$*;Wnt1Cre* (G) and *Osr2*$^{-/-}$*Bmp4*$^{f/-}$*;Wnt1Cre* (H) mutant pups at P0.

Table S1. RNAseq read densities of each of the *Bmp4* exons

Exon	Ctr-max (RPM)	Ctr-man (RPM)	mt-max (RPM)	mt-man (RPM)
4	29.98	30.46	0.21 (0.7%)*	0.18 (0.6%)*
3	3.96	4.92	4.31	4.46
2	1.08	1.51	1.56	2.20
1	1.63	2.08	2.30	2.62

RPM, reads per million mapped reads.
*$P<0.01$ for comparison between control and mutant samples. No significant difference is detected between the maxillary and mandibular molar mesenchyme in either control or mutant samples.

Table S2. RNAseq results for Bmp family ligands

Gene	Ctr-max (RPKM)	Ctr-man (RPKM)	mt-max (RPKM)	mt-man (RPKM)
Bmp2	2.02	4.31	2.26	7.87
Bmp3	17.40	11.84	8.52	4.57
Bmp5	2.60	1.66	0.18	0.10
Bmp6	35.49	33.82	46.73	26.88
Bmp7	3.46	3.38	7.45	4.99
Bmp8a	0.00	0.02	0.00	0.00
Bmp8b	0.57	0.84	0.18	0.40
Bmp10	0.00	0.00	0.00	0.00
Bmp15	0.10	0.00	0.18	0.29

RPKM, reads per kilobase exon per million mapped sequences.

Table S3. Expression profiles of selected genes in maxillary and mandibular mesenchyme

Gene	Ctr-Max	Mt-Max	Ctr-Man	Mt-Man	Ctr-Man vs Ctr-Max		Mt-Max vs Ctr-Max		Mt-Man vs Ctr-Man	
					FC	*P*-value	FC	*P*-value	FC	*P*-value
Dlx6	4.48	3.81	19.78	17.2	4.42	4.36E–07	–1.18	0.65	–1.15	0.67
Wif1	5.52	5.4	13.29	15.72	2.41	8.86E–06	–1.02	0.90	1.18	0.42
Dkk2	9.52	16.37	34.22	63.52	3.59	1.90E–38	1.72	1.23E–04	1.86	5.02E–23
Osr2	92.42	124.03	110.33	177.91	1.19	0.13	1.34	1.81E–05	1.61	5.74E–19

The expression levels shown are in RPKM.
–, downregulation; FC, fold change.